

Study of Ti^{4+} substitution in ZrW_2O_8 negative thermal expansion materials

Klaartje De Buysser^{a,*}, Isabel Van Driessche^a, Bart Vande Putte^b,
Joseph Schaubroeck^b, Serge Hoste^a

^aDepartment of Inorganic and Physical Chemistry, Ghent University, Krijgslaan 281 S-3, B-9000 Ghent, Belgium

^bFaculty of Applied Engineering Sciences, University College Ghent, Schoonmeersstraat 52, B-9000 Ghent, Belgium

Received 2 March 2007; received in revised form 21 May 2007; accepted 30 May 2007

Available online 6 June 2007

Abstract

Powder XRD-analysis and thermo-mechanical analysis on sintered $\text{TiO}_2\text{-WO}_3\text{-ZrO}_2$ mixtures revealed the formation of $\text{Zr}_{1-x}\text{Ti}_x\text{W}_2\text{O}_8$ solid solutions. A noticeable decrease in unit cell parameter 'a' and in the order–disorder transition temperature could be seen in the case of $\text{Zr}_{1-x}\text{Ti}_x\text{W}_2\text{O}_8$ solid solutions.

Studies performed on other ZrW_2O_8 solid solutions have attributed an increase in phase transition temperature to a decrease in free lattice volume, whereas a decrease in phase transition temperature was suggested to be due to the presence of a more disordered state. Our studies indicate that the phase transition temperature in our materials is strongly influenced by the bond dissociation energy of the substituting ion–oxygen bond. A decrease in bond strength may compensate for the effect of a decrease in lattice free volume, lowering the phase transition temperature as the degree of substitution by Ti^{4+} increases. This hypothesis is proved by differential scanning calorimetry.

© 2007 Elsevier Inc. All rights reserved.

Keywords: Negative thermal expansion; Substitution; Phase transition; Calorimetry

1. Introduction

The anharmonicity of the potential well causes positive thermal expansion in most solid materials. However, it is not uncommon for materials to contract upon heating. Examples in this field are tetrahedrally bonded crystals and water at low temperature and β -quartz at high temperatures [1,2]. Most of them show anisotropic negative thermal expansion in a very narrow temperature range. ZrW_2O_8 is a widely examined member of the negative thermal expansion materials. This cubic material exhibits large isotropic negative thermal expansion over a broad temperature range (0–1050 K) [3].

Being part of the AM_2O_8 family, zirconium tungstate is built from ZrO_6 octahedra and WO_4 tetrahedra. The polyhedra are corner linked to one another by shared

oxygen atoms. In the octahedra, all oxygen atoms are bounded to the surrounding tetrahedra, whereas the WO_4 tetrahedra have one free oxygen atom. The polyhedra are part of an open frame work structure. The large negative thermal expansion behaviour is caused by low-energy vibrational–rotational modes of the polyhedra within this open frame work structure. The coupled rotations, without distortion of the intrahedral bond distances or angles, are often referred to as Rigid Unit Modes or RUMs [4–11].

This material has a cubic crystal structure at room temperature with the WO_4 tetrahedra aligned along the [1 1 1] axis. ZrW_2O_8 undergoes a phase transition from cubic α ($P2_13$) to cubic β ($Pa-3$) at 430 K. In the high temperature β -phase, the direction in which the WO_4 tetrahedra point, becomes dynamically disordered. Zirconium tungstate maintains its negative thermal expansion over the α – β -phase transition, but the thermal expansion coefficient becomes smaller (α -phase: $-10 \times 10^{-6} \text{K}^{-1}$; β -phase: $-4 \times 10^{-6} \text{K}^{-1}$) [12]. This order–disorder transition

*Corresponding author. Fax: +3292644983.

E-mail address: Klaartje.DeBuysser@UGent.be (K. De Buysser).

can be easily detected in temperature-dependent X-ray diffraction. The [3 1 0] reflection disappears completely after the α - β -transition. The phase transition temperature can also be seen by thermo-mechanical analysis as α - and β -phases have different thermal expansion coefficients.

There are two different mechanisms published in literature. The first mechanism is a so-called S_N2 reaction in which the free $W_{\text{free}}-O$ bonds are broken followed by an inversion of the tungstate tetrahedra [13]. On the other hand, O^{17} NMR studies have revealed the mechanism behind the phase transition [14]. It was confirmed that all oxygen atoms in the structure are in dynamic exchange even below the phase transition. At the phase transition temperature, adjacent tetrahedra will rotate as a whole in a “ratchet” motion causing mutual exchange between all oxygen sites. This implies breaking of the Zr–O bounds in the Zr–O–W linkages. In that sense, it is clear that substitution of the Zr^{4+} ion within the crystal structure by another ion must strongly affect the phase transition temperature. According to conventional knowledge, the occurrence of substitutional solid solutions requires that the ions that are replacing each other must be similar in size [15]. Another important issue is the charge neutrality of the materials, thereby restricting our choice largely to ions with 4+ valency. Good results concerning solid solutions were obtained by substituting Zr^{4+} ions (86 pm) [16] by other 4+ valency ions such as Sn^{4+} (83 pm) [17] with $0 \leq x \leq 0.2$ and Hf^{4+} (85 pm) with $0 \leq x \leq 1$.

The most widely discussed substituted material is HfW_2O_8 [3,18]. Hafnium tungstate exhibits the same remarkable negative thermal expansion properties as ZrW_2O_8 . The α -phase ($a = 0.9157$ nm) is isostructural with α - ZrW_2O_8 [19]. HfW_2O_8 shows an order–disorder transition at 460 K. Substitution by Sn^{4+} ions induces a decrease in phase transition temperature [17]. In addition to tetravalent substituents, some trivalent ions such as Y^{3+} ($0 \leq x \leq 0.04$), Lu^{3+} ($0 \leq x \leq 0.04$), Sc^{3+} ($0 \leq x \leq 0.04$), In^{3+} ($0 \leq x \leq 0.04$), etc. were also used to prepare substituted ZrW_2O_8 materials [20–24]. Again, the phase transition temperature was affected by the substitution as a decrease in phase transition temperature was noticed.

Substitution of the tungsten ion is most widely studied in $ZrMo_2O_8$. Cubic γ - $ZrMo_2O_8$ is isostructural with β - ZrW_2O_8 [25–27]. Recently, it has been shown that it is possible to prepare $ZrW_{2-x}Mo_xO_8$ phases over the entire composition range $0 \leq x \leq 2$ [28–30]. The phase transition temperature shifts to lower values as the amount of Mo present in the material increases. For example, the $\alpha \rightarrow \beta$ phase transition of $ZrMoWO_8$ is reduced with 160 K compared to the parent compound [31]. The study of shifts in phase transition from α - to β -phase is of great practical importance because it gives the possibility to exclude a phase transition and a disturbing shift in thermal expansion above room temperature.

In this paper, we attempt to substitute Zr^{4+} by Ti^{4+} ions and study the effect of the substitution on the crystal structure and the phase transition temperature. The results

are compared to our earlier published Sn-substituted ZrW_2O_8 materials in order to understand the main parameters affecting the shift in phase transition temperature [17].

2. Experimental

The $Zr_{1-x}Ti_xW_2O_8$ ($x = 0-0.1$) and $Zr_{1-x}Sn_xW_2O_8$ ($x = 0-0.05$) materials were synthesized using a solid state reaction starting from the commercially available oxides ZrO_2 , TiO_2 and SnO_2 (Aldrich). WO_3 was obtained from Acros Organics. The oxide mixtures were co-milled during 24 h in an attrition mill filled with zirconia pearls. The mass ratio of powder:pearls was 1:1. These oxide mixtures were pressed at 750 MPa into small bars of 0.3 g ($2 \text{ mm} \times 2 \text{ mm} \times 13 \text{ mm}$). The bars were sintered during 15 h in a preheated furnace at 1450 K, followed by quenching in liquid nitrogen to avoid decomposition into the metal oxides precursors. The bars were used as such to examine their thermo-mechanical behaviour. The coefficients of thermal expansion and the phase transition temperature were measured with a vertical push rod thermo-mechanical analyser (TA instruments 2940) using a heating rate of 5 K/min from room temperature to 573 K under a constant force of 0.5 N. Differential scanning calorimetry was performed on powder samples using a DSC 2910 (TA Instruments). These measurements were performed under N_2 atmosphere (50 mL/min) between 233 and 573 K at a heating rate of 20 °C/min. Identification of the different phases present in the powder samples was performed on a X-ray diffractometer D5000 using $CuK\alpha$ radiation (Siemens). The XRD powder diffraction data were collected by a step scanning method (2θ range from 10° to 80°). Simultaneous scanning electron microscopy and energy dispersive analysis of X-rays were performed on a FEI-200F (FEI).

3. Results and discussion

The samples of $Zr_{1-x}Ti_xW_2O_8$ ($x = 0-0.1$) and $Zr_{1-x}Sn_xW_2O_8$ ($x = 0-0.05$) were analysed by powder X-ray diffraction to determine the presence of a single phase. The signal:noise ratio was high enough to detect small amounts of crystalline material. As can be seen in Fig. 1, for the $Zr_{1-x}Ti_xW_2O_8$ series, no other reflections besides those belonging to ZrW_2O_8 are present except for the highest degree of substitution in the $Zr_{0.9}Ti_{0.1}W_2O_8$ composition. Here, reflections due to the presence of TiO_2 can be seen. It is hereby proved that this composition exceeds the limit of the solid solution. No reflections of impurity phases can be remarked for the $Zr_{1-x}Sn_xW_2O_8$ series mentioned in Fig. 2. This is a first indication that a solid solution is formed in this range of composition.

SEM–EDX line mapping was used to confirm the homogeneity of the Ti ions among the ZrW_2O_8 matrix. As can be seen in Fig. 3, the signals collected at 10 keV (W L_3 edge) and 5 keV (Ti K edge) are corresponding with

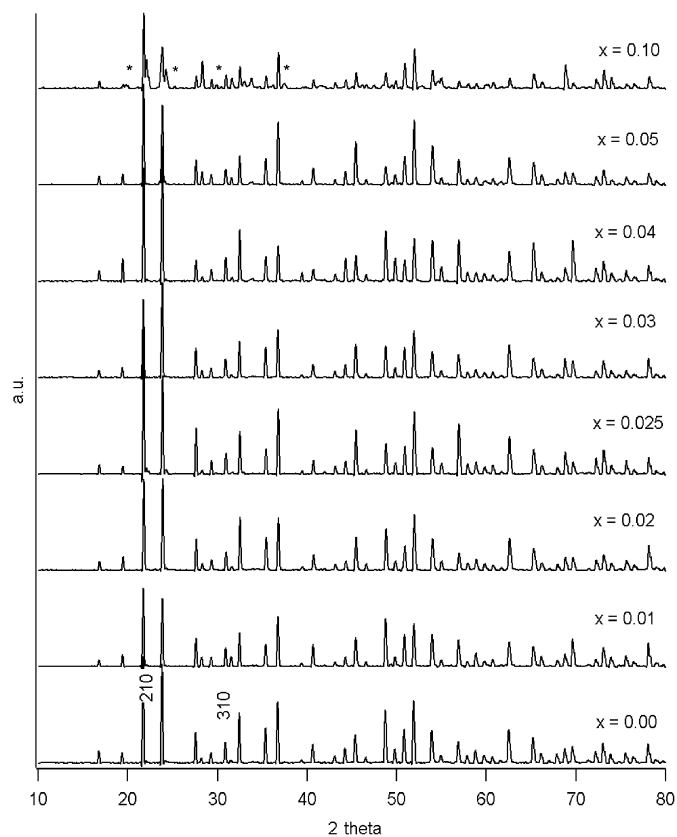


Fig. 1. X-ray diffraction patterns of $Zr_{1-x}Ti_xW_2O_8$ ($x = 0–0.10$) at room temperature (298 K).

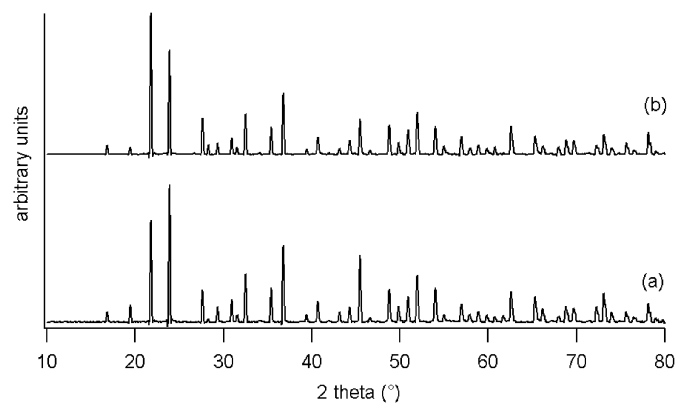


Fig. 2. X-ray diffraction patterns of $Zr_{1-x}Sn_xW_2O_8$: (a) $x = 0.025$ and (b) 0.05 .

each other. The places where both signals drop are associated with pores in the material. Ti can be seen on every spot where a positive signal for the W L edge is obtained. This confirms a homogeneous distribution of the Ti atoms within ZrW_2O_8 necessary to obtain a solid solution.

The influence on the unit cell parameter caused by substitution of the Zr position by cations with a smaller ionic radius was investigated for all the samples mentioned in Figs. 1 and 2. The lattice parameters were calculated using 30 peaks between 30 and 80 2θ by a least-square fit

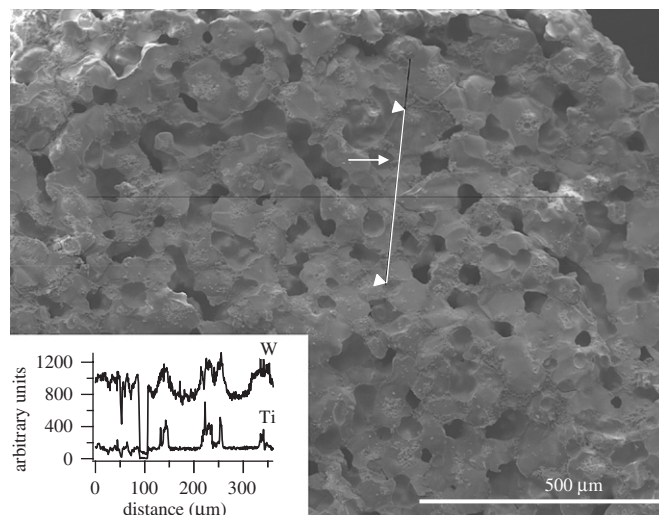


Fig. 3. Line mapping of the Ti and W distribution in $Zr_{0.95}Ti_{0.05}W_2O_8$.

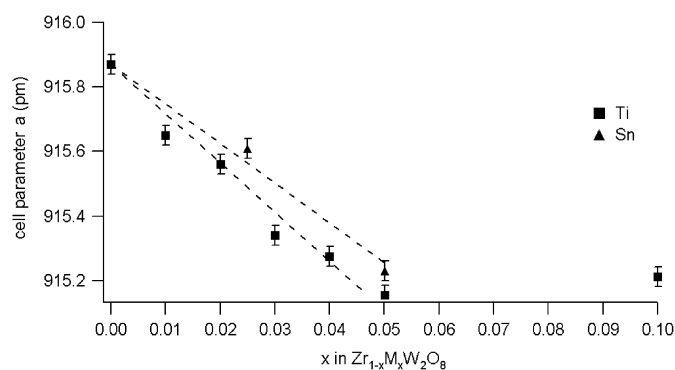


Fig. 4. Lattice parameters of ZrW_2O_8 ($x = 0$), $Zr_{1-x}Ti_xW_2O_8$ ($x = 0.01–0.10$) (\blacktriangle) and $Zr_{1-x}Sn_xW_2O_8$ ($x = 0.025$ and 0.05) (\blacksquare) at 298 K. The linearity according to Vegard's law is indicated by the dotted lines.

after correcting 2θ with Nelson–Riley's method [32]. LaB_6 of 6 wt% was added to the samples as internal standard. Fig. 4 shows the cell parameter 'a' for ZrW_2O_8 , $Zr_{1-x}Ti_xW_2O_8$ ($x = 0.01–0.10$) and $Zr_{1-x}Sn_xW_2O_8$ ($x = 0.025$ and 0.05) at 298 K. For Ti^{4+} and Sn^{4+} , the relative magnitude of the decrease in unit cell parameter is nicely linked to the relative sizes of the substituting ions versus the size of Zr^{4+} . The linear decrease in unit cell parameter with increasing degree of substitution follows Vegard's law [15,17]. The $Zr_{0.9}Ti_{0.1}W_2O_8$ material does not obey this law. The cell parameter of the material does not further decrease in comparison with the 5% substituted material which means that the limit for substitution of Ti^{4+} at the Zr^{4+} position is obtained at 5%, which proves the earlier mentioned observations in XRD-analysis. Materials, which exceed this limit, are not further discussed here.

The decrease of unit cell parameter in the case of Ti and Sn substitution follows the trend that was already reported for substitution with Hf^{4+} [3]. However, these observations are in contrast with the substitution of Zr^{4+} ions by trivalent ions where a decrease of the unit cell parameter is

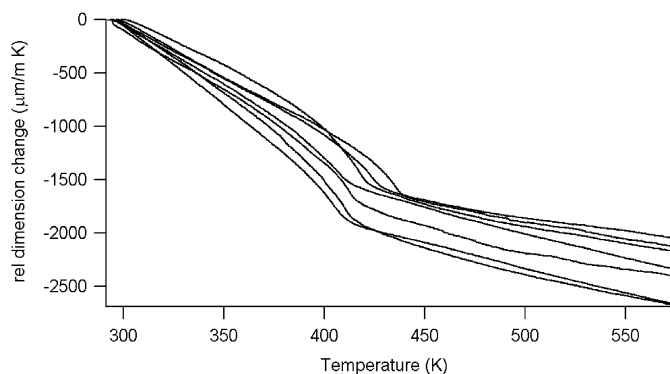


Fig. 5. Relative length differences of sintered $\text{Zr}_{1-x}\text{Ti}_x\text{W}_2\text{O}_8$ ($x = 0.00$ – 0.05) bars as a function of temperature. The top curve is measured on a pure ZrW_2O_8 bar as indicated by (*).

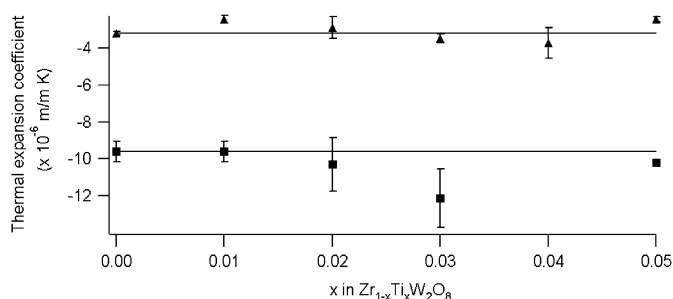


Fig. 6. Thermal expansion coefficients of α - and β - $\text{Zr}_{1-x}\text{Ti}_x\text{W}_2\text{O}_8$.

noticed despite the larger radii. The main reason for this behaviour is the oxygen deficiency, caused by the lower valency of the substituting ions [20]. The substitution by Ti^{4+} and Sn^{4+} respects the electroneutrality of the compound without any need for changes in the oxygen content thus the smaller ionic radius is directly reflected in a decrease in unit cell parameter.

Fig. 5 represents the thermo-mechanical analysis of $\text{Zr}_{1-x}\text{Ti}_x\text{W}_2\text{O}_8$ ($x = 0.00$ – 0.05) samples. The top curve represents a pure ZrW_2O_8 sample. Substitution will not affect the negative thermal expansion properties of the materials. The thermal expansion coefficients of the α - and β -phases of all Ti-substituted materials are plotted in Fig. 6 and no large differences in thermal expansion behaviour can be seen.

The phase transition temperatures of ZrW_2O_8 , $\text{Zr}_{1-x}\text{Ti}_x\text{W}_2\text{O}_8$ ($x = 0.01$ – 0.05) and $\text{Zr}_{1-x}\text{Sn}_x\text{W}_2\text{O}_8$ ($x = 0.025$ and 0.05) were determined by differential scanning calorimetry as the maximum in the anomaly of the heat capacity. The shift in maxima for ZrW_2O_8 , $\text{Zr}_{0.99}\text{Ti}_{0.01}\text{W}_2\text{O}_8$ and $\text{Zr}_{0.98}\text{Ti}_{0.02}\text{W}_2\text{O}_8$ can be seen in Fig. 7 and the phase transition temperatures for all substituted materials are gathered in Fig. 8. The temperature at which the α -phase transforms into the β -phase decreases as the Ti^{4+} -substitution degree increases. Translated into the order-disorder theory this means that with increasing substitution, less thermal energy—reflected in a lower phase transition temperature—is needed to induce the disorder-

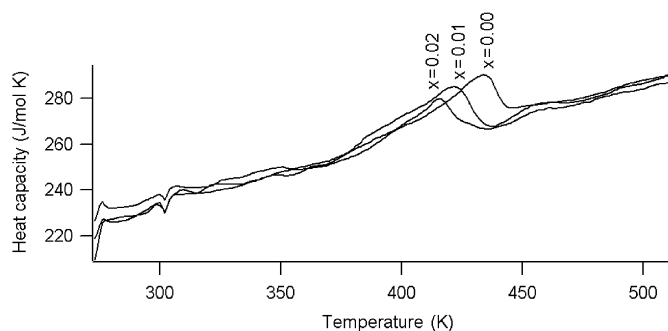


Fig. 7. Heat capacity determined by DSC of ZrW_2O_8 , $\text{Zr}_{0.99}\text{Ti}_{0.01}\text{W}_2\text{O}_8$ and $\text{Zr}_{0.98}\text{Ti}_{0.02}\text{W}_2\text{O}_8$.

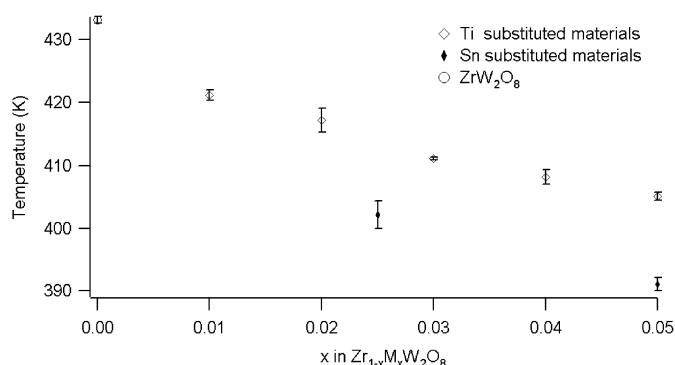


Fig. 8. Phase transition temperatures ZrW_2O_8 ($x = 0$), $\text{Zr}_{1-x}\text{Ti}_x\text{W}_2\text{O}_8$ ($x = 0.01$ – 0.05) (\blacktriangle) and $\text{Zr}_{1-x}\text{Sn}_x\text{W}_2\text{O}_8$ ($x = 0.025$ and 0.05) (\blacksquare).

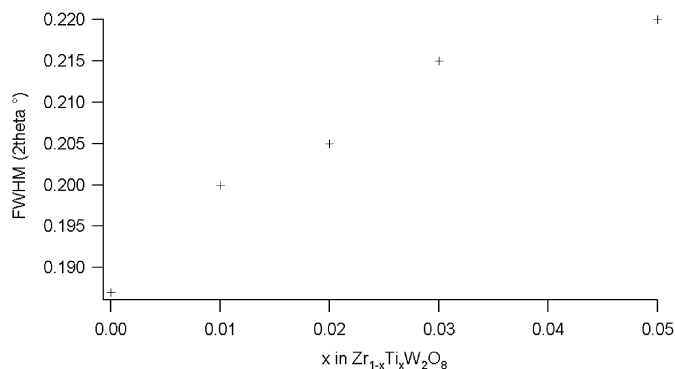


Fig. 9. FWHM calculated for [3 1 0] reflection of $\text{Zr}_{1-x}\text{Ti}_x\text{W}_2\text{O}_8$ ($x = 0$ – 0.05) solid solutions.

ing of the WO_4 tetrahedra. An even more pronounced decrease in phase transition temperature can be noticed for Sn^{4+} -substituted solid solutions. Some authors state that the main reason for the lower phase transition temperature is the presence of a locally disordered state induced by the substituting ion [24]. The disturbance of the periodic order of some WO_4 tetrahedra clusters in the orientationally disordered state in $\text{Zr}_{1-x}\text{Ti}_x\text{W}_2\text{O}_8$ can be confirmed by an increase of the FWHM of the [3 1 0] reflection. An increase in FWHM with 15% was calculated for $\text{Zr}_{1-x}\text{Ti}_x\text{W}_2\text{O}_8$ ($x = 0.00$ – 0.05) samples as given in Fig. 9.

The effect of Hf^{4+} substitution mentioned in literature is in contrast with this latter theory as the phase transition

temperature increases with increasing substitution degree. As explanation for this, it is stated in literature [18] that the phase transition of $Zr_{1-x}Hf_xW_2O_8$ ($x = 0-1$) solid solutions is dependent of the free lattice volume. The free lattice volume is defined as the unit cell volume minus the sum of the volumes for all ions occupying the unit cell. The increase of the phase transition temperature is considered to be due to the decrease of the free space around the WO_4 tetrahedra. To relate our results to the change in free lattice volume, this free lattice volume was calculated for $Zr_{1-x}Ti_xW_2O_8$ ($x = 0.00-0.05$) and plotted against the phase transition temperature (Fig. 10). As can be seen in this figure, the phase transition temperature decreases as the lattice-free volume decreases, which is in contrast with the results mentioned for the Hf^{4+} substitution.

De Meyer et al. [17] have published a phenomenon, which cannot be neglected. The order–disorder transition mechanism, revealed by O^{17} NMR, indicates that during the ratchet motion Zr–O bonds in the Zr–O–W linkages are broken. Substitution of the Zr^{4+} ion by another ion may increase or decrease the bond strength. In Table 1, the ionic radii and bond dissociation energy data are assembled. From this table, it can be seen that the reason for the higher phase transition temperature of Hf-substituted ZrW_2O_8 materials is not only the smaller lattice-free volume but extra evidence can be found in the higher dissociation energy of a Hf–O bond in comparison with a

Zr–O bond as stated in the publication of De Meyer et al. For the Ti^{4+} substitution, however, the lower dissociation energy of the Ti–O bond in comparison with the Zr–O bond will compensate the effect of the smaller lattice-free volume resulting in an overall decrease of the phase transition temperature as the substitution degree increases. The literature data for Y^{3+} and Lu^{3+} also mention a decrease in phase transition temperature, which we can attribute to differences in bond strength. Further confirmation of this phenomenon can be found in the fact that the decrease of phase transition temperature is larger in the case of $Zr_{1-x}Sn_xW_2O_8$ materials than for $Zr_{1-x}Ti_xW_2O_8$ solid solutions due to the higher dissociation energy of Ti–O in comparison with an Sn–O bond.

Differential scanning calorimetry is used to quantify the phase transition enthalpy. As mentioned above, the heat capacity shows an anomaly around the phase transition temperature due to an order–disorder transition. The excess heat capacity is defined as the heat capacity after subtraction of the baseline. The phase transition enthalpy can be calculated as the integration area in which this excess heat capacity can be detected. The phase transition enthalpy for ZrW_2O_8 was experimentally quantified as 490.4 J/mol. This value is smaller than other values (907 J/mol) stated in Ref. [20]. These differences can be understood as originating from another calorimetry technique (DSC versus ASC), baseline calculation and preparation history (presence of quenching effects). The phase transition enthalpies for the Ti-substituted materials are given in Fig. 11. A clear decrease of the phase transition enthalpy can be seen as the substitution degree increases. An increase in phase transition enthalpy after substitution with Hf^{4+} has been reported [19]. Here, we clearly see a decrease because of substitution by Ti^{4+} with a small Ti–O bond strength. This supposes the ratchet motion as the mechanism behind the phase transition. The introduction of less firm bonded ions will only affect the phase transition enthalpy if the Zr–O–W or M–O–W linkages are broken during transition. The substitution of Zr^{4+} by other ions clearly affects the thermo-dynamical parameters involved in the phase transition.

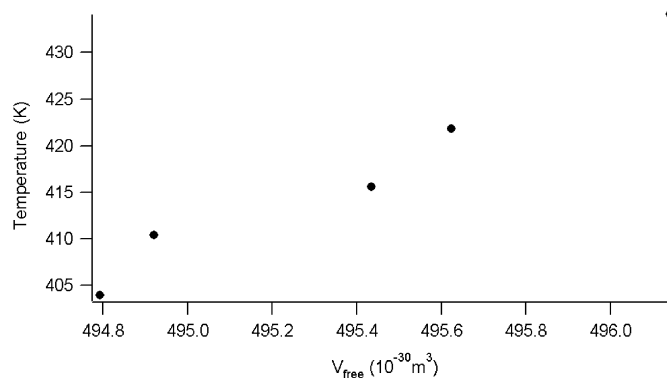


Fig. 10. Phase transition temperatures of $Zr_{1-x}Ti_xW_2O_8$ ($x = 0.00-0.05$) solid solutions versus the calculated lattice free volumes in the unit cell at 298 K.

Table 1

Ionic radii and M–O bond dissociation energies of the substituent ions of the $Zr_{1-x}M_xW_2O_8$ described in this paper

$Zr_{1-x}M_xW_2O_8$ with M:	Ionic radius (pm) [15]	M–O bond dissociation energy (kJ/mol) [33]
Zr^{4+}	86	776.1 ± 9.2
Hf^{4+}	85	801.7 ± 13.4
Sn^{4+}	83	531.8 ± 12.6
Ti^{4+}	74.5	672.4 ± 9.2
Y^{3+}	104	719.6 ± 11.3
Lu^{3+}	100.1	678 ± 8

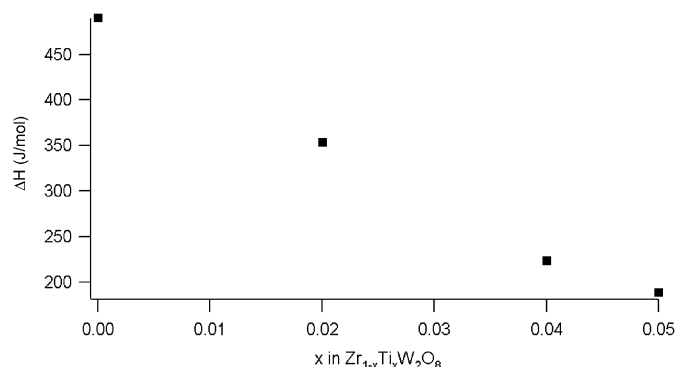


Fig. 11. Phase transition enthalpy for Ti-substituted materials.

4. Conclusion

In this paper, substitution of Zr^{4+} ions by Ti^{4+} resulted in successful synthesis of $Zr_{1-x}Ti_xW_2O_8$ solid solutions with $x = 0.00$ – 0.05 . A decrease in lattice parameters could be identified and was attributed to a smaller ionic radius (74.5 pm) of the substituting metal. The decrease in phase transition temperature noticed in these solid solutions is thought to result from the combination of the presence of a larger disorder state (broadening of the [3 1 0] reflection) and a lower bond dissociation energy of the Ti–O bond in comparison with the Zr–O bond, which compensates for the decrease in lattice-free volume. This phenomenon is proved by differential scanning calorimetry measurements.

Acknowledgments

The authors wish to acknowledge Olivier Janssen at the Department of Solid State Physics, Ghent University, for the collection of X-ray diffraction data and SEM–EDAX analysis.

References

- [1] W.D. Callister, in: W. Anderson (Ed.), *Materials Science and Engineering: An Introduction*, Wiley, Danvers, 2000, pp. 661–664.
- [2] R.E. Taylor, *Thermal Expansion of Solids*, ASM International, 1998, pp. 1–76.
- [3] J.S.O. Evans, et al., *Chem. Mater.* 8 (12) (1996) 2809–2823.
- [4] C.A. Perottoni, J.E. Zorzi, J.A.H. da Jornada, *Solid State Commun.* 134 (5) (2005) 319–322.
- [5] J.S.O. Evans, W.I.F. David, A.W. Sleight, *Acta Crystallogr. Sect. B: Struct. Sci.* 55 (1999) 333–340.
- [6] J.M. Gallardo-Amores, et al., *Int. J. Inorg. Mater.* 2 (1) (2000) 123–129.
- [7] A.W. Sleight, *Inorg. Chem.* 37 (12) (1998) 2854–2860.
- [8] G.D. Barrera, et al., *J. Phys.: Condens. Matter* 17 (4) (2005) R217–R252.
- [9] L.D. Noailles, et al., *Chem. Mater.* 16 (7) (2004) 1252–1259.
- [10] S. Allen, et al., *Acta Crystallogr. Sect. B: Struct. Sci.* 60 (2004) 32–40.
- [11] J.Z. Tao, A.W. Sleight, *J. Solid State Chem.* 173 (2) (2003) 442–448.
- [12] T.A. Mary, et al., *Science* 272 (5258) (1996) 90–92.
- [13] J.S.O. Evans, *J. Chem. Soc. Dalton Trans.* (19) (1999) 3317–3326.
- [14] M.R. Hampson, et al., *Chem. Commun.* (4) (2004) 392–393.
- [15] A.R. West, *Solid solutions*, in: *Solid State Chemistry and Its Applications*, Wiley, Chichester, 1987, pp. 358–374.
- [16] R.D. Shannon, *Acta Crystallogr. Sect. A* 32 (SEP1) (1976) 751–767.
- [17] C. De Meyer, et al., *J. Mater. Chem.* 14 (20) (2004) 2988–2994.
- [18] N. Nakajima, Y. Yamamura, T. Tsuji, *J. Therm. Anal. Calorim.* 70 (2) (2002) 337–344.
- [19] Y. Yamamura, N. Nakajima, T. Tsuji, *Phys. Rev. B* 6418 (18) (2001) (part. no. 184109).
- [20] T. Tsuji, Y. Yamamura, N. Nakajima, *Thermochim. Acta* 416 (1–2) (2004) 93–98.
- [21] T. Hashimoto, et al., *Solid State Commun.* 131 (3–4) (2004) 217–221.
- [22] N. Nakajima, Y. Yamamura, T. Tsuji, *Solid State Commun.* 128 (5) (2003) 193–196.
- [23] Y. Morito, et al., *J. Ceram. Soc. Jpn.* 110 (9) (2002) 807–812.
- [24] Y. Yamamura, M. Kato, T. Tsuji, *Thermochim. Acta* 431 (1–2) (2005) 24–28.
- [25] C. Lind, et al., *J. Mater. Chem.* 11 (12) (2001) 3354–3359.
- [26] C. Lind, et al., *Chem. Mater.* 10 (9) (1998) 2335–2337.
- [27] S. Allen, J.S.O. Evans, *Phys. Rev. B* 68 (13) (2003).
- [28] C. Closmann, A.W. Sleight, J.C. Haygarth, *J. Solid State Chem.* 139 (2) (1998) 424–426.
- [29] L. Huang, et al., *Eur. J. Inorg. Chem.* (22) (2005) 4521–4526.
- [30] U. Kameswari, A.W. Sleight, J.S.O. Evans, *Int. J. Inorg. Mater.* 2 (4) (2000) 333–337.
- [31] J.S.O. Evans, et al., *J. Am. Chem. Soc.* 122 (36) (2000) 8694–8699.
- [32] J.B. Nelson, D.P. Riley, *Proc. Phys. Soc.* 57 (3) (1945) 160.